Characteristics and drivers of plant virus community spatial patterns in U.S. West Coast grasslands

Amy E. Kendig, Elizabeth T. Borer, Charles E. Mitchell, Alison G. Power, and Eric W. Seabloom

A. Kendig (kend0110@umn.edu, orcid.org/0000-0002-2774-1795), E. Borer, and E. Seabloom, Dept of Ecology, Evolution, and Behavior, University of Minnesota, St. Paul, MN 55108, USA. – C. Mitchell, Curriculum for the Environment and Ecology and Dept of Biology, University of North Carolina at Chapel Hill, Chapel Hill, NC 27599, USA. – A. Power, Dept of Ecology and Evolutionary Biology, Cornell University, Ithaca, NY 14853, USA.

The formatted version of this article can be found here:
https://onlinelibrary.wiley.com/doi/10.1111/oik.04178

Abstract

The spatial distribution of disease risk caused by multi-pathogen infections is not frequently characterized, limiting understanding of the drivers of infection and thwarting prediction of future risk in a changing environment. Further complicating this predictive understanding is that interactions among multiple pathogens within a host commonly alter transmission success, infection risk, and disease dynamics. By characterizing spatial patterns of Barley and Cereal Yellow Dwarf Virus (B/CYDV) infections that range from the scale of an individual plant to thousands of neighboring plants, we examined the contributions of spatial processes to the distribution of disease risk. In a two-year field experiment, we planted grass hosts of B/CYDVs into fertilized plots of U.S. west coast grasslands. We determined how vector-sharing, environmental conditions, and spatial variation in host quality affected spatial patterns of single viruses, pairs of viruses, and the whole virus community across out-planted grass hosts. We found that single viruses and virus communities were spatially random, indicating that infection does not solely spread through the community in a wave-like manner. On the other hand, we found that pairs of viruses, especially those that share a vector species, were aggregated spatially. This suggests that if within-host competition exists, it is not strong. Aggregation in one pair of viruses was more frequent due to environmental conditions and spatial variation in out-planted host quality, measured as vector preference. These results highlight the importance of insect vectors for predicting the spatial distribution of coinfection risk by B/CYDVs.

Key words: barley and cereal yellow dwarf viruses, disease ecology, insect-vectored plant pathogens

Introduction

Multi-pathogen infections can increase virulence and alter disease dynamics relative to single infections (Graham et al. 2007, Griffiths et al. 2011). While spatial patterns of disease risk are used to infer valuable information about disease spread, such as the mode of transmission, the distance between transmission events, and spatial variation in hosts or environmental conditions (Caraco et al. 2001, Jolles et al. 2002, Kikuti et al. 2015, Nessa et al. 2015), they are not well characterized for multi-pathogen infections (but see Raybould et al. 1999, Turechek and Madden 2000, Muller and van Woesik 2012). However, spatial patterns of communities of free-living organisms have been well studied and are influenced by dispersal, biotic interactions, and environmental heterogeneity (Bolker and Pacala 1999, Hanson et al. 2012, Benot et al. 2013). Recent applications of community ecology theory to multi-pathogen communities demonstrate that analogous processes (transmission, pathogen interactions, and variation in the host community) mediate the diversity of co-infecting pathogens within a host individual or population (Seabloom et al. 2015, Johnson et al. 2016, Mordecai et al. 2016). Therefore, it is likely that transmission, pathogen interactions, and spatial variation in hosts also contribute to the spatial patterns of pathogen communities, but the roles and strengths of these processes are unclear.

The distance and mode of transmission between hosts likely influence the spatial patterns of multi-pathogen communities. If transmission of a single pathogen is localized, infection tends to be aggregated across hosts (i.e. infected hosts tend to be geographically close to other infected hosts, leading to spatially clustered occurrences of infection). However, if transmission is coming from a distant source, infection tends to be spatially random (Gibson 1997, Filipe and Maule 2004). Building on this, areas with higher initial prevalence have more local sources of infection, so they are more likely to have aggregations of infection (Jolles et al. 2002, Rappussi et al. 2012). If multiple species in a community have localized dispersal, communities that are geographically close to one another tend to have more similar species composition (i.e. the distance-decay relationship, Nekola and White 1999). Transmission mode also may affect the spatial patterns of pathogen communities. For example, the spatial patterns of pathogens vectored by insects are influenced by foraging behavior (McElhany et al. 1995, Ferrari et al. 2006). Different pathogens can share the same mode of transmission, such as insects or needles, which may lead to aggregation between these pathogens (Ridzon et al. 1997, Manguin et al. 2010, Hersh et al. 2014).

Interactions among pathogens also can determine whether different pathogens are aggregated relative to one another, or regularly spaced (i.e. segregated from one another, like a checkerboard pattern). While facilitation between different free-living species causes aggregation, and competition leads to regular spatial patterns (Callaway 1995, Seabloom et al. 2005), the spatially continuous nature of these interactions does not easily extend to obligate pathogens. Pathogens can have facilitative or competitive interactions, but these are typically mediated through host resources or the immune system (Pedersen and Fenton 2007). In addition, the extent that pathogens overlap in their host specificity determines the frequency with which they will interact (Brisson and Dykhuizen 2004, Malpica et al. 2006, Johnson et al. 2016). Therefore, pathogens that successfully infect the same hosts and have positive or neutral interactions are expected to aggregate while those with different host “preferences” or negative interactions are

expected to segregate. However, these patterns are restricted to the scale of a host individual or smaller, as the presence of a pathogen in one host is unlikely to affect the presence of a different pathogen in a different host.

Multiple factors, including genetics, nutrition, healthcare, and environmental conditions, affect host susceptibility and competence, measures of host quality. Overlap in host quality requirements among pathogens can contribute to the distance-decay relationship of pathogen communities if there is a spatial gradient in host quality (Bell 2010, King et al. 2010, Astorga et al. 2012). For single pathogens, spatial variation in genetic resistance has been linked to aggregation of infection (Laine 2006, Paull et al. 2012). Disease risk caused by single infections and coinfections also can be affected by spatially variable environmental conditions that alter host susceptibility or pathogen fitness (Jarosz and Burdon 1988, Raso et al. 2006, Kikuti et al. 2015). Localized transmission and low competitive exclusion among pathogens must work in tandem with spatial variation in host quality for pathogen communities to be aggregated (Leibold et al. 2004, Seabloom et al. 2005, Hanson et al. 2012).

Here, we use a grassland experiment, repeated over two years, to evaluate the role of spatial processes in structuring an aphid-vectored plant virus community. We planted six grass species into plots with full-factorial nitrogen (N) and phosphorus (P) fertilization for a growing season (Borer et al. 2010b, Seabloom et al. 2013). We quantified spatial variation in the host quality of out-planted grasses through plant size and aphid feeding preference. Using the infection status of out-planted grasses for four viruses, we characterized the spatial patterns of single virus species, pairs of virus species, and the whole virus community within experimental plots. We tested if these spatial patterns could be explained by spatial variation in host quality and two environmental conditions that drive plot-scale infection prevalence (fertilization and perennial grass cover, Borer et al. 2010b). We did not observe aggregation of single infections or the virus community, which would have indicated strictly localized transmission. However, we did find close associations among virus pairs, suggesting the importance of shared aphid vectors in determining the spatial patterns of this plant virus community.

Methods

Experimental system

A group of plant viruses known as the Barley and Cereal Yellow Dwarf viruses (B/CYDVs) are an ideal study system for investigating spatial patterns of pathogen communities. Their stationary hosts make the characterization of spatial patterns straightforward, and the ecology of these pathogens has been well studied (Power et al. 2011). They can infect over 150 species of perennial and annual grasses, including crops and wild grasses (D'Arcy and Burnett 1995). The virus species included in this study are BYDV-MAV, BYDV-PAV, CYDV-RPV, and BYDV-RMV (henceforth MAV, PAV, RPV, and RMV, respectively). Each virus is obligately vectored by a different aphid species, except PAV, which shares one vector species with RPV (*Rhopalosiphum padi*) and two with MAV (*Sitobian avenae* and *Metopolophium dirhodum*) (Power et al. 2011). However, facilitation during coinfection allows viruses to be vectored by aphids that they are typically incompatible with (Wen and Lister 1991). Within-host pathogen interactions can also be competitive (Wen et al. 1991), and they may depend on soil nutrient content (Lacroix et al. 2014). Hosts that are fast-growing tend to have high susceptibility and

134 competence (Cronin et al. 2010), which is why the mass of out-planted grasses are
135 approximations for host quality. Aphids typically walk between plants or make flights of
136 a few meters, but they have the ability to fly tens of kilometers with wind assistance
137 (Parry 2013).
138 *Field experiment*
139 The experiment was repeated in two years (2007 and 2008). In the first year, sites
140 included the Hopland Research and Extension Center (39°N, 123°W), the McLaughlin
141 Natural Reserve (38.8°N, 122.3°W), and the Sierra Foothill Research and Extension
142 Centers (38.7°N, 121.1°W) in California, USA. In the second year, two more sites in
143 Oregon were added: Baskett Slough National Wildlife Refuge (44.9°N, 122.7°W) and
144 William L. Finley National Wildlife Refuge (44.4°N, 122.6°W). Two experimental blocks
145 were established at each site with four 40 m x 40 m plots within each block (Fig. A1).
146 The plots in each block received a factorial combination of nitrogen (N, 10 g m^{-2} $year^{-1}$
147 added quarterly as calcium nitrate) and phosphorus (P, 4.3 g m^{-2} $year^{-1}$ added quarterly as
148 triple super phosphate) addition (plot-level treatments: control, +N, +P, or +N and P).
149 Fertilizers were first applied to plots in December 2006, one month prior to the first
150 planting. We estimated aerial cover of naturally-occurring plant species in two 0.5 m x 1
151 m quadrats within each plot. Cover of each species was estimated separately such that the
152 combined cover could exceed 100%.
153 Within each plot, 10 transects were established with 20 subplots each. Transects were
154 spaced 4 m apart and the centers of subplots were 2 m apart along each transect (Fig.
155 A1). Each year, 2-3 transects per plot were randomly selected to be used in the
156 experiment. In January 2007 and 2008, after approximately one month of growth in a
157 greenhouse, we planted six individual plants of different species in the subplots of these
158 selected transects. All subplots received the same six species. The plants were spaced
159 0.25 m apart parallel to the transect and 0.2 m apart perpendicular to the transect (Fig.
160 A1). Three phylogenetic groups are represented by the six species, which are common to
161 West Coast grasslands. For each phylogenetic group, one species is an exotic annual and
162 one is a native perennial, respectively: Brome (*Bromus hordeaceus/Bromus carinatus*),
163 Oat (*Avena fatua/Koeleria macrantha*), and Rye (*Taeniatherum caput-medusae/Elymus*
164 *glaucus*). The plants were randomly assigned to a position within each subplot (i.e. A
165 through E in Fig. A1). The out-planted grasses were in the field prior to seasonal aphid
166 flight and harvested before the onset of senescence, in late May and early June. Post-
167 harvest, we shipped all green tissue overnight to labs at Cornell University and the
168 University of North Carolina to test them for the presence of MAV, PAV, and RPV in
169 2007, and MAV, PAV, RPV, and RMV in 2008 with double antibody sandwich enzyme-
170 linked immunosorbent assay (DAS-ELISA). Plants tested for viruses were individually
171 weighed in 2008. These analyses resulted in a dataset of over 3000 plants from the first
172 experimental year and over 5000 plants from the second year. Data are available from the
173 Dryad Digital Repository: http://dx.doi.org/10.5061/dryad.22dt8 (Borer et al. 2010a).
174 *General approach for characterizing spatial patterns*
175 Spatial correlograms are nonparametric statistical tools used to quantify associations
176 among individual units (i.e. autocorrelation) across geographical distances (Bjørnstad and
177 Falck 2001). Similarly, spatial cross-correlograms estimate distance-based cross-
178 correlations between units representing two different groups, and multivariate
179 correlograms estimate compositional similarity or dissimilarity across space (e.g. the

Mantel correlogram) (Bjørnstad and Falck 2001). We used spatial correlograms to characterize spatial variation in host quality and spatial patterns of viruses within out-planted grasses. Based on the planting layout described above, we assigned spatial coordinates to all out-planted grasses. Coordinates accurately represented the space between plants within each plot, but were set such that spatial associations between plants from different plots would not be evaluated. We used the spline.correlog function in the ncf package in R to build spatial correlograms (Bjørnstad 2016). For all correlograms, we used df = 15, a maximum lag distance of 30 m (to include 85% of the pairwise comparisons), and 1000 permutations to calculate 95% confidence intervals (CI) through bootstrapping. We chose to use df=15 because this roughly corresponds to 15 distance classes (Bjørnstad et al. 1999), which is appropriate for our experimental set-up. However, variation in the df can modify the outcome of our analyses (Appendix 2).

After we fit spatial correlograms to host quality data and virus infection data, we used the output of these correlograms as predictor variables and response variables, respectively, in linear regressions. The spline.correlog function provides estimates for the y-intercept (i.e. correlation at the scale of a single plant) and the x-intercept (i.e. the geographic distance at which the correlation is no longer significantly different from zero) of each correlogram. When the 95% CI included the origin, we categorized the correlogram as "random". When the y-intercept was significantly positive, we categorized the correlogram as "aggregated", and when the y-intercept was significantly negative, we categorized it as "regular". To reduce the carryover of error in estimating spatial correlograms to analyses with linear regressions, we used 0 or 1 to represent whether the spatial correlogram was random or significantly different from random rather than the x- or y-intercepts.

In U.S. west coast grasslands, most, if not all, grasses are potential hosts to B/CYDVs. We present some of our results in units of individual plants to estimate the number of hosts that are affected by the disease. To convert geographic distances from meters to number of individual plants, we used measurements from common annual and perennial grass species in a restored grassland at the Sedgwick Natural Reserve in California, USA, which is ecologically similar to the grasslands in our study (Seabloom et al. 2005). The basal radius, averaged across plant species from Sedgwick, is 1.52 cm and the average maximum radius is 11.69 cm. To estimate the number of plants included in an aggregate, the x-intercept of the correlogram was assumed to be the diameter of a circle. Based on the values from Sedgwick, experimental plots encompass approximately one million to ten million individual plants, depending on the sizes of plants.

Characterizing spatial patterns of host quality

Spatial variation in host quality was characterized by creating correlograms of two metrics for each experimental plot: host mass and aphid preference. We created correlograms of host mass using the wet mass of each out-planted grass following harvest in the second experimental year (data were not collected the first year). While these data may show a spatial pattern, we acknowledge that non-experimental host plants may not adhere to this pattern due to variation in age and species. We used laboratory experiments of aphid preference with the species *R. padi* to assign each out-planted grass an aphid preference value based on its species (Experiment III in Borer et al. 2009). These values and the corresponding plant positions in the field were used to build correlograms of aphid preference. Because one of each plant species is in each subplot, these

correlograms are affected by experimental design. However, they may also be influenced by less predictable factors, such as the random placement of species within a subplot and individual survival over the growing season.

Characterizing spatial patterns of viruses

We used correlograms to characterize the spatial pattern of each virus species based on presence or absence in each out-planted grass. We used cross-correlograms to characterize the relative spatial patterns between virus species pairs and multivariate correlograms to analyze community-wide spatial patterns, both relying on presence/absence data. We reduced the df to 7 and removed permutations that caused errors in the multivariate correlogram due to low infection prevalence, which did not affect the overall results.

Evaluating drivers of virus spatial patterns

Coinfection may drive aggregation between virus pairs when local transmission from coinfected plants occurs, particularly in the presence of mutualistic interactions. In addition, positive y-intercepts of cross-correlograms may result from coinfection, although they can be interpolated from positive associations between adjacent plants as well. Conversely, spatial aggregation of virus pairs can increase coinfection rates by making transmission of virus pairs to the same plant individual more likely. Because we cannot disentangle cause and effect when examining coinfection and cross-correlograms, we compared these metrics using Pearson's correlation coefficient. We examined the relationship between x-intercepts of significantly aggregated cross-correlograms and the relative coinfection rate for each pair of viruses in each plot . Relative coinfection rate measures the rate of coinfection relative to what is expected due to chance encounters between viruses. It was calculated by the plot-scale coinfection rate minus the product of each virus's plot-scale prevalence (modification of Malpica et al. 2006). We chose the relative coinfection rate rather than the raw coinfection rate because cross-correlograms indicate whether pairs of viruses co-occur more often than expected by chance.

Next, we evaluated the effects of a shared transmission route (i.e. the same vector species) on whether or not aggregation occurred between each virus pair in each experimental plot, with aggregation determined by a cross-correlogram having a significantly positive y-intercept. We fit a generalized linear mixed-effects model to the relationship between whether or not aggregation occurred and whether or not the virus pair share the same vector (R package lme4, Bates et al. 2015). The initial random effects were the identity of the viruses nested within plot nested within block nested within site nested within state, which reduced down to virus identities nested within site based on backwards stepwise model selection with likelihood ratio tests (Crawley 2007).

Then, we assessed the effects of N addition, P addition, the interaction between N and P addition, perennial grass percent cover, spatial variation in plant mass, and spatial variation in aphid preference on whether or not aggregation between virus pairs occurred with generalized linear regressions. We built separate models for each virus pair in each year. Models for the first year did not include spatial variation in plant mass or perennial cover (most CA plots had no perennial grasses). Each host quality variation metric (aphid preference and plant mass) was represented by a 1 or 0 for each experimental plot, indicating the presence or absence, respectively, of a significant correlogram y-intercept (i.e. significant aggregation or segregation). We began by building mixed-effects models with block nested within site nested within state (for the second experimental year) as the

random effects. We used backwards stepwise selection with likelihood ratio tests for model simplification of random effects, then fixed effects (Crawley 2007). The fixed-effects models were significantly better than the mixed-effects models for the first experimental year and we had issues with model convergence for mixed-effects models from the second experimental year, so only the fixed-effects models were used. All statistical analyses were performed in R version 3.3.1 (R Core Team 2016).

Results

Spatial patterns of host quality: random patterns of grass mass and regular patterns of aphid preference

Spatial correlograms of out-planted host mass revealed random spatial patterns in more than 80% of plots, with local aggregation occurring in six out of 35 plots (Table 1). On the other hand, plants with similar aphid preference scores had regular spatial patterns in most plots and random patterns in a minority of plots (Table 1). The average distance of segregation between plants with similar aphid preference scores was about the distance between subplots along a transect (2.0 m), indicating that aphid preference segregation was driven by experimental design and likely represents plant species differences. These differences are not strictly constrained to be aphid preference because, as we measured it, this is a species-specific trait.

Single virus spatial patterns were predominantly random

Spatial patterns of single pathogens provide insights about the scale of transmission (i.e. more localized transmission leads to aggregation) and spatial variation in host quality. Contrary to expectations, most virus spatial correlograms depicted random patterns (Fig. A3). There were three exceptions to this trend, all from the first experimental year: RPV had two negative correlograms and PAV had one (Fig. A4). The x- and y-intercepts of these correlograms are close to those found for aphid preference (Table 1), indicating that the patterns were likely to be driven by differences among plant species, potentially due to characteristics such as aphid preference or susceptibility to infection.

Aggregated spatial patterns of virus pairs were related to coinfection and vector-sharing, but only one pair was affected by environmental conditions and spatial variation in host quality

Cross-correlograms between pathogens are influenced by transmission, interactions between pathogens, and overlapping host quality requirements. The cross-correlograms between pairs of B/CYDV species indicated either random or aggregated spatial patterns, but none were regular (Table 2, Fig. A3). Across both experimental years, aggregation between virus pairs occurred out to 3.93 ± 0.46 m on average, which encompasses approximately 10,000 to 80,000 plants. Significantly positive y-intercepts occurred at least once for every virus pair, but the average of these intercepts was somewhat low (correlation of 0.1671 ± 0.0070). This indicates that the net interactions between virus pairs are either positive or neutral with aggregation driven by shared transmission routes or overlapping host quality preferences between virus species.

We compared the cross-correlogram length to the relative coinfection rate to evaluate how much aggregation between virus pairs relates to coinfection and, potentially, transmission from coinfected plants. We expected a positive relationship between these metrics due to overlapping biological processes. We found that in both years, aggregation

between virus pairs only occurred above a threshold relative coinfection rate, but without a clear linear relationship beyond this threshold (Pearson's r = -0.11, p=0.59; Pearson's r = 0.02, p=0.92 for years one and two, respectively; Fig. 1). Therefore, it is likely that some minimum rate of coinfection is required for aggregation between viruses to occur, consistent with the concept that the y-intercept of cross-correlograms represents coinfection. However, spatial relationships between viruses beyond a single host are independent of coinfection rate.

There were only enough virus pairs to statistically evaluate the effect of a shared transmission route (i.e. the same vector species) on aggregation between viruses in the second experimental year. As expected, virus pairs that share a vector species aggregated more frequently than those that do not (p=0.003, Fig. 2b, Table A5). This result arose despite high frequency of aggregation between one pair of viruses that do not share a vector, RPV and MAV (Fig. 2).

We also investigated the effects of two environmental conditions that increase prevalence (plot-scale nutrient addition and perennial grass percent cover) and two metrics of spatial variation in out-planted host quality (aphid preference and plant mass) on the aggregation of virus pairs. For all pairs involving RMV, aggregation only occurred in one to two plots, preventing model convergence. During the second experimental year, the frequency of aggregation between PAV and RPV increased when there was significant segregation between out-planted grasses based on aphid preference (p=0.02; Fig. 3a, Table A6). Also in the second experimental year, perennial grass percent cover (p=0.005, Fig 3b, Table A6) and P addition (p=0.007, Fig. 3c, Table A6) increased aggregation of PAV and RPV. We found no significant effects of these environmental conditions or spatial variation in host quality on the aggregation of other virus pairs in the second experimental year or any virus pairs in the first year.

Virus community spatial patterns were random

Multivariate correlograms indicate whether within-host pathogen communities are more similar in geographically closer plants, and how this relationship decays with distance. They can be influenced by transmission, pathogen interactions, and spatial variation in host quality. The spatial pattern of the B/CYDV community was random for every experimental plot in both experimental years, indicating that geographically closer plants do not have more similar virus communities. Because MAV and RPV frequently aggregated despite not sharing a vector (Fig. 2), we suspected that the aggregation of MAV and RPV may have been caused by shared aggregation with PAV, but the multivariate correlograms of these three viruses when RMV was removed from the dataset were still random.

Discussion

Here we presented a unique spatial analysis of multiple pathogens vectored by multiple aphid species in a diverse host environment. Our results complement growing knowledge about drivers of pathogen community diversity (Seabloom et al. 2015). While the out-planted grass hosts were species commonly found in U.S. West Coast grasslands, they may differ from the background plant community in characteristics relevant to B/CYDV spread, so we refrain from extrapolating our results to this background community or naturally-occurring grasslands in general. Spatial patterns of single virus species and the virus community were random among out-planted grasses, which

suggests that infection did not solely spread in a wave-like manner from a small set of initial points. Rather, at least some transmission events occurred between non-neighboring plants (Filipe and Maule 2004). In addition, virus pairs were frequently aggregated relative to each other, and this rate was even higher for those that share a vector species. Finally, spatial variation among out-planted hosts, quantified here by aphid preference, and environmental factors that increase prevalence contributed to aggregation between one pair of viruses, but did not influence the others. Forms of spatial heterogeneity that we did not measure may contribute to aggregation between these other pairs. Nonetheless, frequent aggregation between virus pairs at the scale of an individual host indicates that within-host competition, if it exists, is not strong. Together, these results suggest that aphid-vectored transmission and a lack of intense competition contributed to aggregation of virus pairs, but, despite expectations, strictly local transmission, measures of spatial variation in host quality, and environmental conditions that increase prevalence often did not affect virus spatial patterns.

We expected that aggregation of infection would arise from aphids walking between plants (Power 1991, Parry 2013) and environmental conditions that increase disease prevalence and local inoculum (Jolles et al. 2002, Rappussi et al. 2012). However, we found almost all spatial patterns of single viruses were random. Spatial patterns of virus pairs also provided evidence that transmission is not likely to be strictly localized. We expected coinfection to increase aggregation between virus pairs in geographically close plants due to localized transmission, particularly when facilitative interactions, such as heterologous encapsidation (i.e. when the RNA from one virus is encased in the protein coat of another), occurred (Wen and Lister 1991). A minimum rate of coinfection was necessary for aggregation to occur, but more coinfected plants did not lead to extended aggregation between viruses. While there is evidence for local dispersal of B/CYDVs from “spillover” hosts (Power and Mitchell 2004), this and other studies showing plant disease aggregation often occur in assemblages of low plant diversity (Sone et al. 2012, Nessa et al. 2015). Natural grasslands and other highly diverse ecological environments are likely to obscure aggregation caused by localized dispersal through mechanisms such as variation in host quality, vector foraging preferences, and the initial spatial distribution of disease inoculum (Caraco et al. 2001, Medel et al. 2004, Ferrari et al. 2006, Gosme and Lucas 2011). Regardless of diversity, longer-lived plants can accumulate infections over time, resulting in random spatial patterns of disease (Raybould et al. 1999). Our experiment controlled the age of out-planted grasses, but not that of plants in the surrounding community.

While sources of local inoculum did not lead to aggregation of single viruses in the out-planted grasses, they may have increased aggregation between PAV and RPV. Previous analyses on these data demonstrated that P addition increases the prevalence of PAV and perennial grass cover increases the prevalences of both PAV and RPV (Seabloom et al. 2013). Presumably, these factors increase viral prevalence in out-planted grass hosts through increased prevalence in the background grass community. P addition may increase the maintenance of infection, as some viruses require an environment with high P concentrations for replication (Clasen and Elser 2007). Perennial grasses are expected to serve as refuges for B/CYDVs between growing seasons (Mckirdy and Jones 1993, Power et al. 2011). Given the generality of these mechanisms, it is surprising that only one pair of viruses was affected by environmental conditions. This may be due to

variation across virus species in response to P addition or their ability to maintain long-term infection in perennial hosts (Mckirdy and Jones 1993, Lacroix et al. 2014). The effect of local inoculum on pathogen spatial patterns has primarily been evaluated for single pathogen species (Jolles et al. 2002, Rappussi et al. 2012). We expect that higher inoculum levels can increase the co-occurrence of pathogens with positive interactions or aggregating forces, particularly when disease prevalence is low. However, spatially explicit models of multi-pathogen communities are necessary to solidify this hypothesis.

The high frequency of aggregation between viruses that share a vector suggests that viruses are either co-transmitted by the same vector individual, or individuals within the same vector species have similar foraging behavior and are spatially aggregated. In addition, the finding that PAV and RPV tend to be more aggregated when grasses preferred by their aphid vector are regularly spaced suggests that *R. padi* transmitted both viruses to highly preferred plants, which is consistent with a previous analysis of this dataset (Seabloom et al. 2013). The relative influence of co-transmission and sequential transmission depends on pathogen interactions with one another and their vector. For example, *Babesia microti* and *Borrelia burgdorferi* have facilitative interactions and are frequently found together in their shared tick vector, *Ixodes scapularis* (Dunn et al. 2014, Hersh et al. 2014). On the other hand, *Anopheles* spp. mosquitoes can transmit *Plasmodium* spp. and *Wuchereria bancrofti*, but co-transmission of these pathogens leads to decreased transmission and mosquito survival, suggesting that sequential transmission is more likely to occur than co-transmission (Manguin et al. 2010). The latter example is relevant for PAV, which has decreased transmission when a vector has previously acquired MAV (Gildow and Rochow 1980). On the other hand, facilitation through heterologous encapsidation may contribute to the high rate of aggregation between MAV and RPV, which do not share a vector (Wen and Lister 1991). Interestingly, the strong effect of shared dispersal mechanisms on community spatial patterns has also been demonstrated for plants with animal-dispersed seeds (Mellado and Zamora 2016, Wright et al. 2016).

Many communities of free-living microbes show patterns consistent with the distance-decay relationship (Hanson et al. 2012). Often, spatial heterogeneity in the environment has a stronger influence on the distance-decay relationship in these communities than dispersal limitation (Bell 2010, King et al. 2010, Astorga et al. 2012). However, B/CYDV communities were spatially random, suggesting that neither dispersal limitation nor environmental gradients are strong in this system at the scales we measured. In many systems, variation among hosts is assumed to affect disease spread through processes such as the dilution effect (Ostfeld and Keesing 2012). Therefore, it is striking that, with the exception of PAV and RPV, we did not find evidence for the influence of spatial variation in host quality on B/CYDV spatial patterns. Heterogeneity in host quality may be structuring B/CYDV communities at different scales than those we examined. For example, transmission events between neighboring plants and small aggregates of plants favorable to aphids or infection may not have been detected by our analyses. In addition, the scale of environmental heterogeneity likely to drive the distance-decay relationship for B/CYDVs may be larger than an experimental plot. For instance, perennial grass cover increases prevalence for three B/CYDV species, and there is more variation in this factor across regions than there is across meters (Borer et al. 2010b, Seabloom et al. 2013). Experimental manipulation of host quality at varying

scales would help clarify the extent to which host heterogeneity influences the spatial structure of pathogen communities.

Given that some processes that generate spatial co-occurrence of virus pairs also are likely to cause aggregation of single viruses and virus communities, it is surprising that we saw aggregation in the former, but not the latter two. For example, overlapping preference for a spatially aggregated host characteristic would be expected to increase aggregation of all three (Seabloom et al. 2005, King et al. 2010). However, cross-correlograms assess the relative spatial patterns of two entities while correlograms and multivariate correlograms measure the autocorrelation of a single entity (either one virus species or a particular composition of viruses) over space (Bjørnstad and Falck 2001). Therefore, co-occurrence of virus pairs in the same plant, same subplot, or neighboring subplots can lead to significant cross-correlograms, but will not necessarily affect the other two forms of virus spatial patterns. A similar result was found for viruses in *Brassica*, with random spatial patterns of each of the four viruses, but positive associations between most of the virus pairs at the scale of a single plant (Raybould et al. 1999). On the other hand, two fungal diseases were found to each have aggregated spatial patterns in strawberry fields while they had low spatial associations with one another (Turechek and Madden 2000). These limited examples suggest that the pathogen type and mode of transmission may be important for understanding the differences among single and multiple plant pathogen spatial patterns.

Due to the complexity of our system, the experimental results incorporate various ecological interactions, providing a meaningful contribution to the rising understanding of pathogen community spatial patterns. The strong signal of co-transmission in pathogen spatial patterns highlights vector control as a coinfection management strategy. While the effects of co-transmission are analogous to effects of co-dispersal observed for free-living organisms (Mellado and Zamora 2016, Wright et al. 2016), pathogen-specific factors can shape pathogen community spatial patterns as well. Importantly, pathogen spatial patterns are intrinsically linked with other living organisms – their hosts. In fact, virulence-induced mortality and behavioral changes due to infection can affect disease patterns (Vasconcelos et al. 1996, Muller and van Woesik 2012). Additionally, ecological interactions between hosts and other organisms can modify spatial patterns of disease (Byers et al. 2008). As we have demonstrated here, the study of pathogen community spatial patterns provides important insights for disease management and a platform to draw comparisons between the ecology of pathogens and free-living organisms.

Acknowledgments

The work presented here would not have been possible without the support of many people and organizations. Marty Dekkers, Burl Martin, Emily Orling, Jasmine Peters, Vincent Adams, the 2006-2008 field crews, and many students were responsible for the data collection. Staff of the University of California Reserve System, University of California Research and Extension Centers, and the U.S. Fish and Wildlife Service provided generous support. Support was provided, in part, by NSF/NIH EID grants EF-0525666 and DEB-1015805 to ETB and EWS, EF-0525641 and DEB-1015909 to CEM, and EF-0525669 and DEB-1015903 to AGP. AEK was supported by an NSF IGERT graduate fellowship at the University of Minnesota (DGE-0653827) and an NSF Graduate Research Fellowship (base award number 0006595).

References

Astorga, A. et al. 2012. Distance decay of similarity in freshwater communities: do macro- and micro- organisms follow the same rules? - Glob. Ecol. Biogeogr. 21: 365–75.

Bates, D. et al. 2015. Fitting linear mixed-effects models using {lme4}. - J. Stat. Softw. 67: 1–48.

Bell, T. 2010. Experimental tests of the bacterial distance-decay relationship. - ISME J. 4: 1357–65.

Benot, M.-L. et al. 2013. Fine-scale spatial patterns in grassland communities depend on species clonal dispersal ability and interactions with neighbours. - J. Ecol. 101: 626–636.

Bjørnstad, O. N. 2016. ncf: Spatial Nonparametric Covariance Functions. - R Packag. version: 1.1-4.

Bjørnstad, O. N. and Falck, W. 2001. Nonparametric spatial covariance functions: Estimation and testing. - Environ. Ecol. Stat. 8: 53–70.

Bjørnstad, O. N. et al. 1999. Synchrony and scaling in dynamics of voles and mice in northern Japan. - Ecology 80: 622–637.

Bolker, B. M. and Pacala, S. W. 1999. Spatial moment equations for plant competition: Understanding spatial strategies and the advantages of short dispersal. - Am. Nat. 153: 575–602.

Borer, E. T. et al. 2009. Aphid fecundity and grassland invasion: invader life history is the key. - Ecol. Appl. 19: 1187–96.

Borer, E. et al. 2010a. Data from: Local context drives infection of grasses by vector-borne generalist viruses. - Dryad Digit. Repos.

Borer, E. T. et al. 2010b. Local context drives infection of grasses by vector-borne generalist viruses. - Ecol. Lett. 13: 810–8.

Brisson, D. and Dykhuizen, D. E. 2004. ospC diversity in Borrelia burgdorferi: different hosts are different niches. - Genetics 168: 713–22.

Byers, J. E. et al. 2008. Controls of spatial variation in the prevalence of trematode parasites infecting a marine snail. - Ecology 89: 439–51.

Callaway, R. M. 1995. Positive interactions among plants. - Bot. Rev. 61: 306–349.

Caraco, T. et al. 2001. Host spatial heterogeneity and the spread of vector-borne infection. - Theor. Popul. Biol. 59: 185–206.

Clasen, J. L. and Elser, J. J. 2007. The effect of host Chlorella NC64A carbon:phosphorus ratio on the production of Paramecium bursaria Chlorella Virus-1. - Freshw. Biol. 52: 112–122.

Crawley, M. 2007. The R Book. - John Wiley & Sons, Ltd.

Cronin, J. P. et al. 2010. Host physiological phenotype explains pathogen reservoir potential. - Ecol. Lett. 13: 1221–1232.

D'Arcy, C. J. and Burnett, P. A. 1995. Barley Yellow Dwarf: 40 Years of Progress. - The American Phytopathological Society.

Dunn, J. M. et al. 2014. Borrelia burgdorferi promotes the establishment of Babesia microti in the northeastern United States. - PLoS One 9: e115494.

Ferrari, M. J. et al. 2006. A gravity model for the spread of a pollinator-borne plant pathogen. - Am. Nat. 168: 294–303.

Filipe, J. A. N. and Maule, M. M. 2004. Effects of dispersal mechanisms on spatio-

548 temporal development of epidemics. - J. Theor. Biol. 226: 125–141.
549 Gibson, G. J. 1997. Investigating mechanisms of spatiotemporal epidemic spread using
550 stochastic models. - Phytopathology 87: 139–146.
551 Gildow, F. and Rochow, W. 1980. Transmission interference between two isolates of
552 barley yellow dwarf virus in Macrosiphum avenae. - Phytopathology 70: 122–126.
553 Gosme, M. and Lucas, P. 2011. Effect of host and inoculum patterns on take-all disease
554 of wheat incidence, severity and disease gradient. - Eur. J. Plant Pathol. 129: 119–
555 131.
556 Graham, A. L. et al. 2007. Transmission consequences of coinfection: cytokines writ
557 large? - Trends Parasitol. 23: 284–91.
558 Griffiths, E. C. et al. 2011. The nature and consequences of coinfection in humans. - J.
559 Infect. 63: 200–6.
560 Hanson, C. A. et al. 2012. Beyond biogeographic patterns: processes shaping the
561 microbial landscape. - Nat. Rev. Microbiol. 10: 497–506.
562 Hersh, M. H. et al. 2014. Co-infection of blacklegged ticks with Babesia microti and
563 Borrelia burgdorferi is higher than expected and acquired from small mammal hosts.
564 - PLoS One 9: 9–13.
565 Jarosz, A. M. and Burdon, J. J. 1988. The effect of small-scale environmental changes on
566 disease incidence and severity in a natural plant-pathogen interaction. - Oecologia
567 75: 278–281.
568 Johnson, P. T. J. et al. 2016. Habitat heterogeneity drives the host-diversity-begets-
569 parasite-diversity relationship: evidence from experimental and field studies. - Ecol.
570 Lett. 19: 752–761.
571 Jolles, A. E. et al. 2002. Disease transmission of Aspergillosis in sea fans: Inferring
572 process from spatial pattern. - Ecology 83: 2373–8.
573 Kikuti, M. et al. 2015. Spatial distribution of dengue in a Brazilian urban slum setting:
574 Role of socioeconomic gradient in disease risk. - PLoS Negl. Trop. Dis. 9: 1–18.
575 King, A. J. et al. 2010. Biogeography and habitat modelling of high-alpine bacteria. -
576 Nat. Commun. 1: 53.
577 Lacroix, C. et al. 2014. Environmental nutrient supply alters prevalence and weakens
578 competitive interactions among coinfecting viruses. - New Phytol. 204: 424–433.
579 Laine, A.-L. 2006. Evolution of host resistance: looking for coevolutionary hotspots at
580 small spatial scales. - Proc. R. Soc. B Biol. Sci. 273: 267–273.
581 Leibold, M. A. et al. 2004. The metacommunity concept: a framework for multi-scale
582 community ecology. - Ecol. Lett. 7: 601–613.
583 Malpica, J. M. et al. 2006. Association and host selectivity in multi-host pathogens. -
584 PLoS One 1: e41.
585 Manguin, S. et al. 2010. Review on global co-transmission of human Plasmodium species
586 and Wuchereria bancrofti by Anopheles mosquitoes. - Infect. Genet. Evol. 10: 159–
587 177.
588 McElhany, P. et al. 1995. Vector preference and disease dynamics: a study of barley
589 yellow dwarf virus. - Ecology 76: 444–457.
590 Mckirdy, S. J. and Jones, R. A. C. 1993. Occurrence of Barley Yellow Dwarf Virus
591 serotypes MAV and RMV in over-summering grasses. - Aust. J. Agric. Res. 44:
592 1195–1209.
593 Medel, R. et al. 2004. Effects of vector behavior and host resistance on mistletoe

aggregation. - Ecology 85: 120–126.
Mellado, A. and Zamora, R. 2016. Spatial heterogeneity of a parasitic plant drives the seed-dispersal pattern of a zoochorous plant community in a generalist dispersal system. - Funct. Ecol. 30: 459–467.
Mordecai, E. a. et al. 2016. Within-host niche differences and fitness trade-offs promote coexistence of plant viruses. - Am. Nat. 187: E13–E26.
Muller, E. M. and van Woesik, R. 2012. Caribbean coral diseases: Primary transmission or secondary infection? - Glob. Chang. Biol. 18: 3529–3535.
Nekola, J. C. and White, P. S. 1999. The distance decay of similarity in biogeography and ecology. - J. Biogeogr. 26: 867–878.
Nessa, B. et al. 2015. Spatial pattern of natural spread of rice false smut (Ustilaginoidea virens) disease in fields. - Am. J. Agric. Biol. Sci. 10: 63–73.
Ostfeld, R. S. and Keesing, F. 2012. Effects of host diversity on infectious disease. - Annu. Rev. Ecol. Evol. Syst. 43: 157–182.
Parry, H. R. 2013. Cereal aphid movement: general principles and simulation modelling. - Mov. Ecol. 1: 14.
Paull, S. H. et al. 2012. From superspreaders to disease hotspots: Linking transmission across hosts and space. - Front. Ecol. Environ. 10: 75–82.
Pedersen, A. B. and Fenton, A. 2007. Emphasizing the ecology in parasite community ecology. - Trends Ecol. Evol. 22: 133–9.
Power, A. G. 1991. Virus spread and vector dynamics in genetically diverse plant populations. - Ecology 72: 232–241.
Power, A. G. and Mitchell, C. E. 2004. Pathogen spillover in disease epidemics. - Am. Nat. 164: S79–S89.
Power, A. G. et al. 2011. The community ecology of barley/cereal yellow dwarf viruses in Western US grasslands. - Virus Res. 159: 95–100.
R Core Team 2016. R: A language and environment for statistical computing.: http://www.R-project.org/.
Rappussi, M. C. C. et al. 2012. Cauliflower stunt associated with a phytoplasma of subgroup 16SrIII-J and the spatial pattern of disease. - Eur. J. Plant Pathol. 133: 829–840.
Raso, G. et al. 2006. An integrated approach for risk profiling and spatial prediction of Schistosoma mansoni-hookworm coinfection. - PNAS 103: 6934–9.
Raybould, A. F. et al. 1999. The prevalence and spatial distribution of viruses in natural populations of Brassica oleracea. - New Phytol. 141: 265–275.
Ridzon, R. et al. 1997. Simultaneous transmission of human immunodeficiency virus and hepatitise C virus from a needle-stick injury. - N. Engl. J. Med. 336: 919–922.
Seabloom, E. W. et al. 2005. Spatial signature of environmental heterogeneity, dispersal, and competition in successional grasslands. - Ecol. Monogr. 75: 199–214.
Seabloom, E. W. et al. 2013. Richness and composition of niche-assembled viral pathogen communities. - PLoS One 8: e55675.
Seabloom, E. W. et al. 2015. The community ecology of pathogens: coinfection, coexistence and community composition. - Ecol. Lett. 18: 401–415.
Sone, K. et al. 2012. Spatial distribution pattern of pine trees killed by pine wilt disease in a sparsely growing, young pine stand. - J. Plant Stud. 2: 1–6.
Turechek, W. W. and Madden, L. V 2000. Analysis of the association between the

640 incidence of two spatially aggregated foliar diseases of strawberry. - Phytopathology
641 90: 157–70.
642 Vasconcelos, S. D. et al. 1996. Modified behavior in baculovirus-infected lepidopteran
643 larvae and its impact on the spatial distribution of inoculum. - Biol. Control 7: 299–
644 306.
645 Wen, F. and Lister, R. M. 1991. Heterologous encapsidation in mixed infections among
646 four isolates of barley yellow dwarf virus. - J. Gen. Virol. 72: 2217–23.
647 Wen, F. et al. 1991. Cross-protection among strains of barley yellow dwarf virus. - J.
648 Gen. Virol. 72: 791–9.
649 Wright, S. J. et al. 2016. Interspecific associations in seed arrival and seedling
650 recruitment in a Neotropical forest. - Ecology 97: 2780–2790.
651

652 Tables

653 Table 1. Summary of correlograms by experimental plot for metrics of spatial vairaiton in
654 host quality, which were used as predictor variables in analyses that follow. Prop. sig. is
655 the proportion of experimental plots with significant y-intercepts.

Host heterogeneity metric	Expt. year	Prop. sig.	Mean ± std. error of sig. x-int. (m)	Mean ± std. error of sig. y-int. (m)
Individual plant mass	2	6/35	8.1 ± 2.0	0.381 ± 0.062
Aphid preference	1	22/24	2.03 ± 0.20	-0.2217 ± 0.0050
Aphid preference	2	27/35	1.839 ± 0.068	-0.2119 ± 0.0054

656

Table 2. Summary of cross-correlograms by experimental plot for virus pairs. Prop. sig. is the proportion of experimental plots with significant cross-correlations.

Virus Pair	Expt. year	Prop. sig.	Mean ± std. error of sig. x-int. (m)	Mean ± std. error of sig. y-int. (m)
MAV-PAV	1	7/24	4.2 ± 1.2	0.140 ± 0.015
MAV-PAV	2	17/34	3.6 ± 1.1	0.194 ± 0.019
MAV-RPV	1	14/24	4.4 ± 1.2	0.162 ± 0.012
MAV-RPV	2	13/34	4.3 ± 1.2	0.167 ± 0.016
MAV-RMV	2	1/34	1.4	0.146
PAV-RPV	1	6/24	6.1 ± 2.0	0.1107 ± 0.0062
PAV-RPV	2	15/35	3.2 ± 0.88	0.188 ± 0.017
PAV-RMV	2	2/35	2.3 ± 0.28	0.154 ± 0.037
RPV-RMV	2	2/35	1.8 ± 0.49	0.1072 ± 0.0066

Figure Legends

Figure 1. The length of the cross-correlation for each virus pair in each plot against their relative coinfection rate (see main text for details) (A) for the first experimental year (Pearson's r = -0.11, p=0.59) and (B) the second (Pearson's r = 0.02, p=0.92). Each virus pair is represented by a different symbol: ● MAV-PAV, ○ MAV-RPV, ■ PAV-RPV, □ MAV-RMV, △ PAV-RMV, and ▽ RPV-RMV.

Figure 2. The mean proportion of experimental plots with positive y-intercepts (with 95% CI) for each virus pair, coded by whether or not they share a vector (A) for the first experimental year and (B) the second. Vector-sharing increased the rate of aggregation in the second experimental year (p=0.003).

Figure 3. The effect of (A) whether or not there is segregation among out-planted hosts based on their aphid preference values (p=0.02), (B) perennial grass cover (p=0.006), and (C) P addition (p=0.007) on aggregation between PAV and RPV in the second experimental year. In (B), points are data, jittered along the y-axis by 0.05, and the line represents predicted probabilities based on the simplest generalized linear model. (A) and (C) are the mean proportion of experimental plots with positive y-intercepts (with 95% CI), determined from the data.

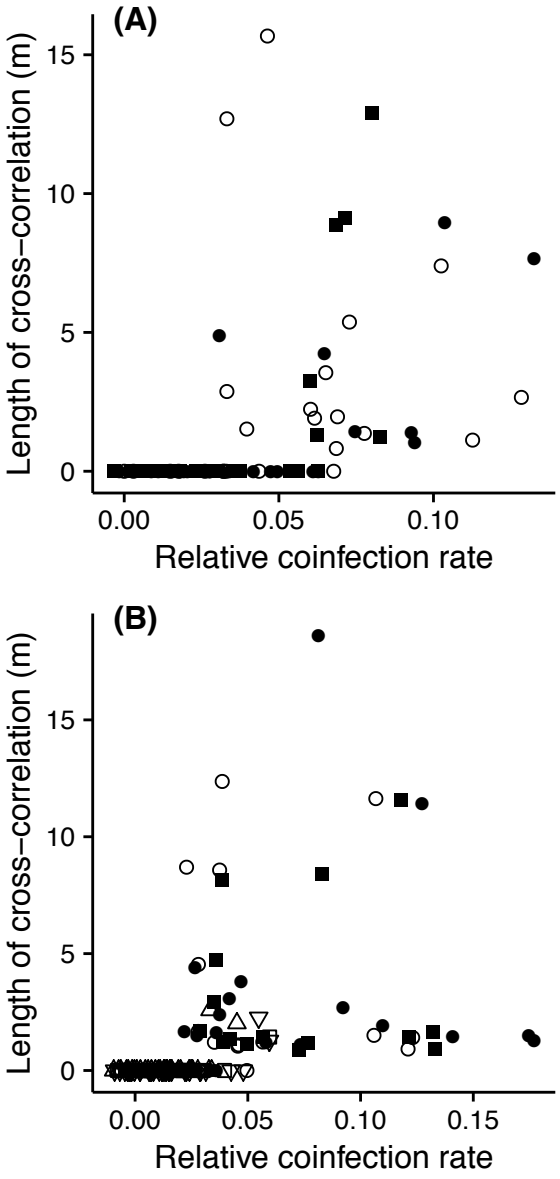
(A)
Length of cross−correlation (m)
15
10
5
0
0.00
0.05
0.10
Relative coinfection rate
(B)
Length of cross−correlation (m)
15
10
5
0
0.00
0.05
0.10
0.15
Relative coinfection rate

681

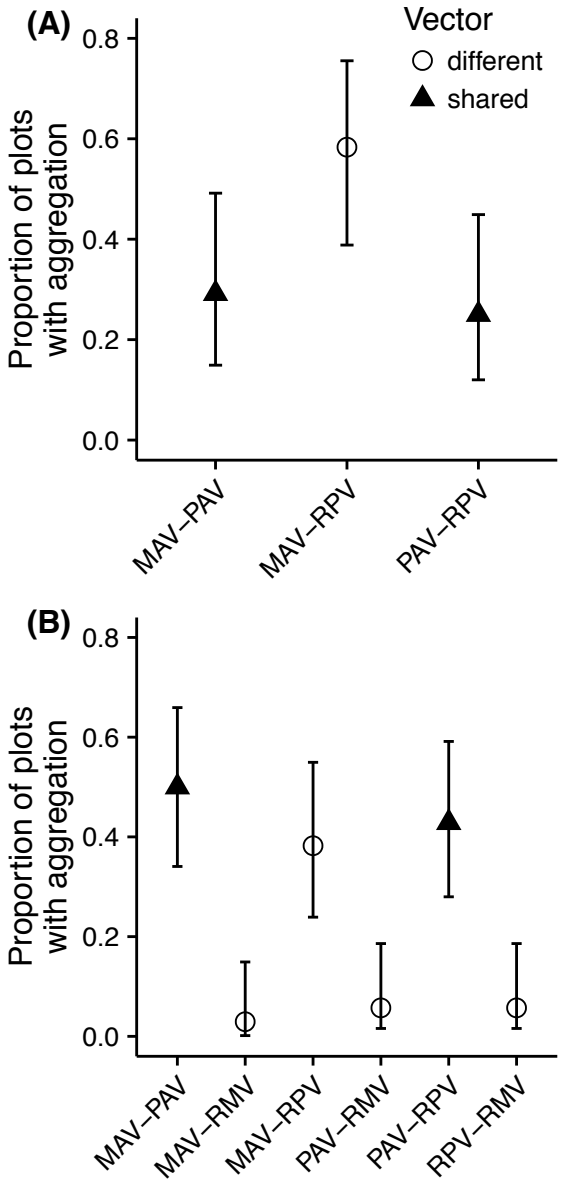
(A)
Vector
different
shared
Proportion of plots with aggregation
0.0
0.2
0.4
0.6
0.8
MAV–PAV
MAV–RPV
PAV–RPV
(B)
Proportion of plots with aggregation
0.0
0.2
0.4
0.6
0.8
MAV–PAV
MAV–RMV
MAV–RPV
PAV–RMV
PAV–RPV
RPV–RMV

682

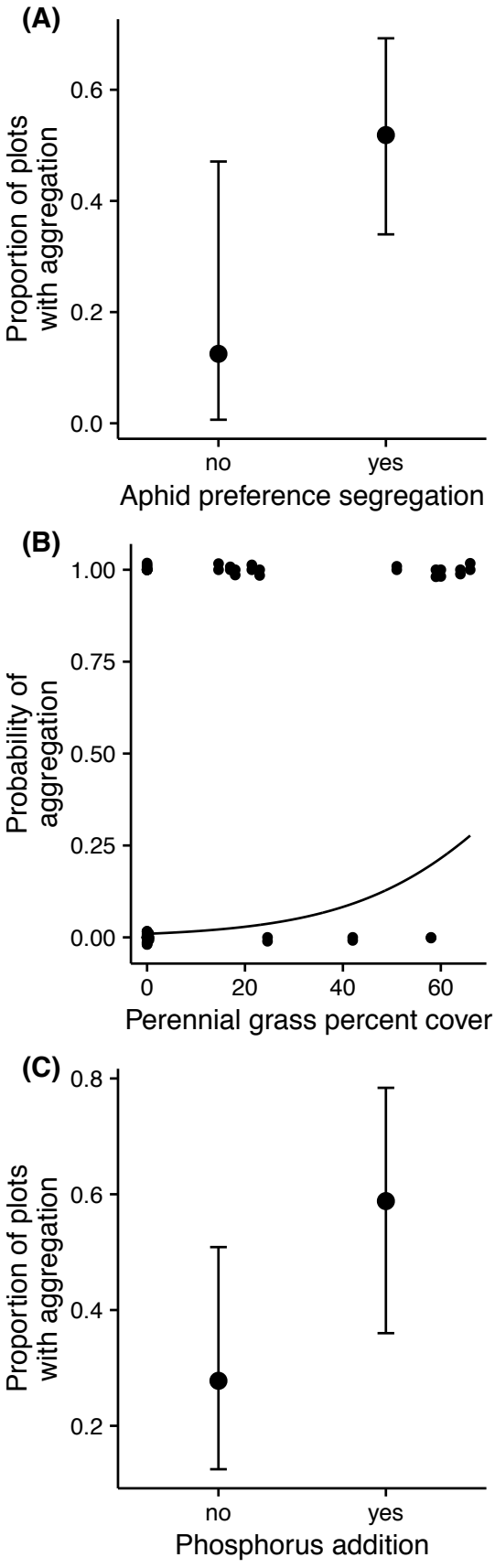
(A)
Proportion of plots with aggregation
0.0
0.2
0.4
0.6
no
yes
Aphid preference segregation
(B)
Probability of aggregation
0.00
0.25
0.50
0.75
1.00
0
20
40
60
Perennial grass percent cover
(C)
Proportion of plots with aggregation
0.2
0.4
0.6
0.8
no
yes
Phosphorus addition

683

Appendix 1: Experimental design

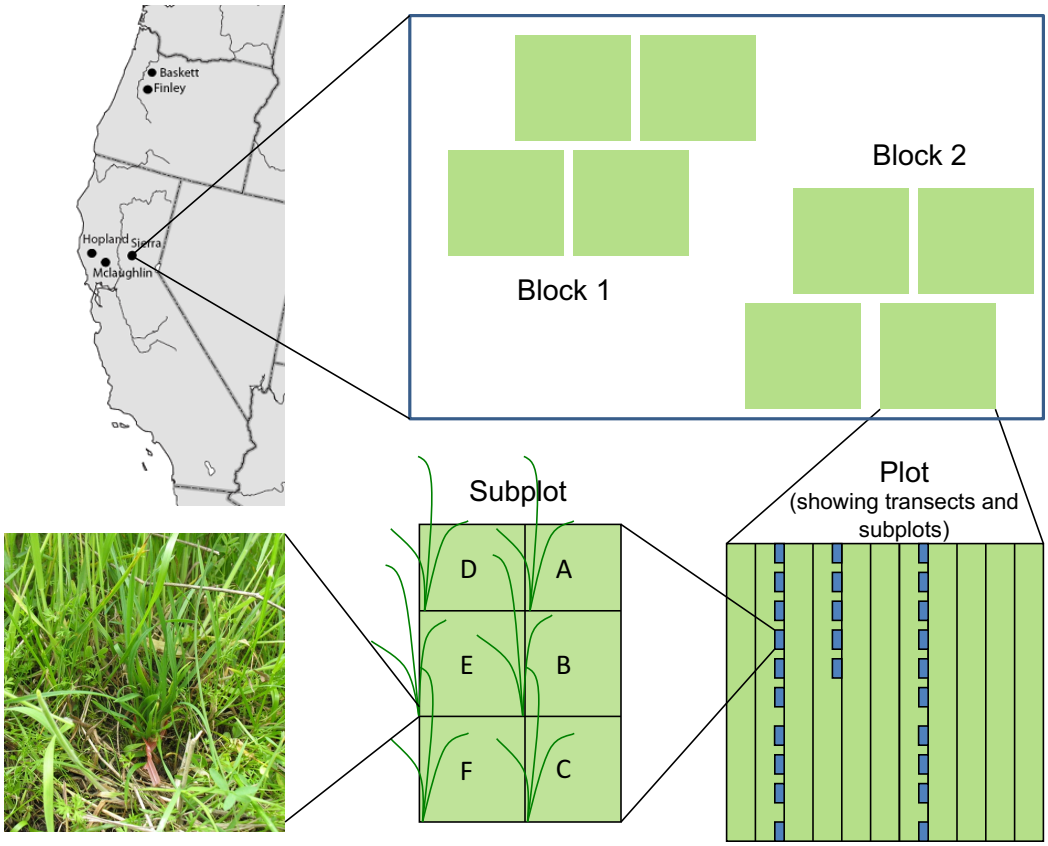

Figure A1. The spatially nested experimental design. Individual grasses were planted into locations A-E of subplots, which were arranged along transects across a plot. Four plots were in each block, with each plot receiving a different nutrient addition treatment. Each site had two blocks. Three sites ae located in California and two are in Oregon. Figure re-published with permission from Borer et al. 2010, Ecology Letters (doi: 10.1111/j.1461-0248.2010.01475.x). Copyright © 1999 - 2016 John Wiley & Sons, Inc. All Rights Reserved.

693 Appendix 2: Effects of correlogram df settings
694 The df setting for the spline correlogram function (Bjørnstad 2016), which we used to
695 analyze spatial variation in host quality and the spatial patterns of infection, can change
696 the outcome of our analyses. Results presented in the main text use df=15. When df = 20,
697 the x-intercepts of cross-correlations are generally smaller and there are slightly fewer
698 significant cross-correlations (compare Table A2 to Table 2, main text). In addition, the
699 effect of vector-sharing on aggregation (Fig. 2, Table A5) and the effects of perennial
700 grass cover and spatial variation in aphid preference on the frequency of PAV and RPV
701 aggregation (Fig. 3a, Table A6) were found to be significant in models with df = 20 while
702 the effect of P addition (Fig. 3c, Table A6) on PAV and RPV aggregation was not.
703
704 Table A2. Summary of cross-correlations by experimental plot for virus pairs when
705 df=20 for the spline correlogram settings. Prop. sig. is the proportion of experimental
706 plots with significant cross-correlations.

Virus Pair	Expt. year	Prop. sig.	Mean ± std. error of sig. x-int. (m)	Mean ± std. error of sig. y-int. (m)
MAV-PAV	1	6/24	0.684 ± 0.025	0.1898 ± 0.0088
MAV-PAV	2	18/34	2.20 ± 0.17	0.2382 ± 0.0044
MAV-RPV	1	15/24	2.37 ± 0.18	0.1944 ± 0.0033
MAV-RPV	2	13/34	2.47 ± 0.27	0.2125 ± 0.0048
PAV-RPV	1	7/24	2.05 ± 0.46	0.1438 ± 0.0025
PAV-RPV	2	15/35	2.30 ± 0.22	0.2326 ± 0.0052
MAV-RMV	2	2/34	0.86 ± 0.16	0.141 ± 0.020
PAV-RMV	2	2/35	1.90 ± 0.29	0.175 ± 0.029
RPV-RMV	2	4/35	2.28 ± 0.57	0.1334 ± 0.0084

707
708

Appendix 3: Virus correlograms and cross-correlograms

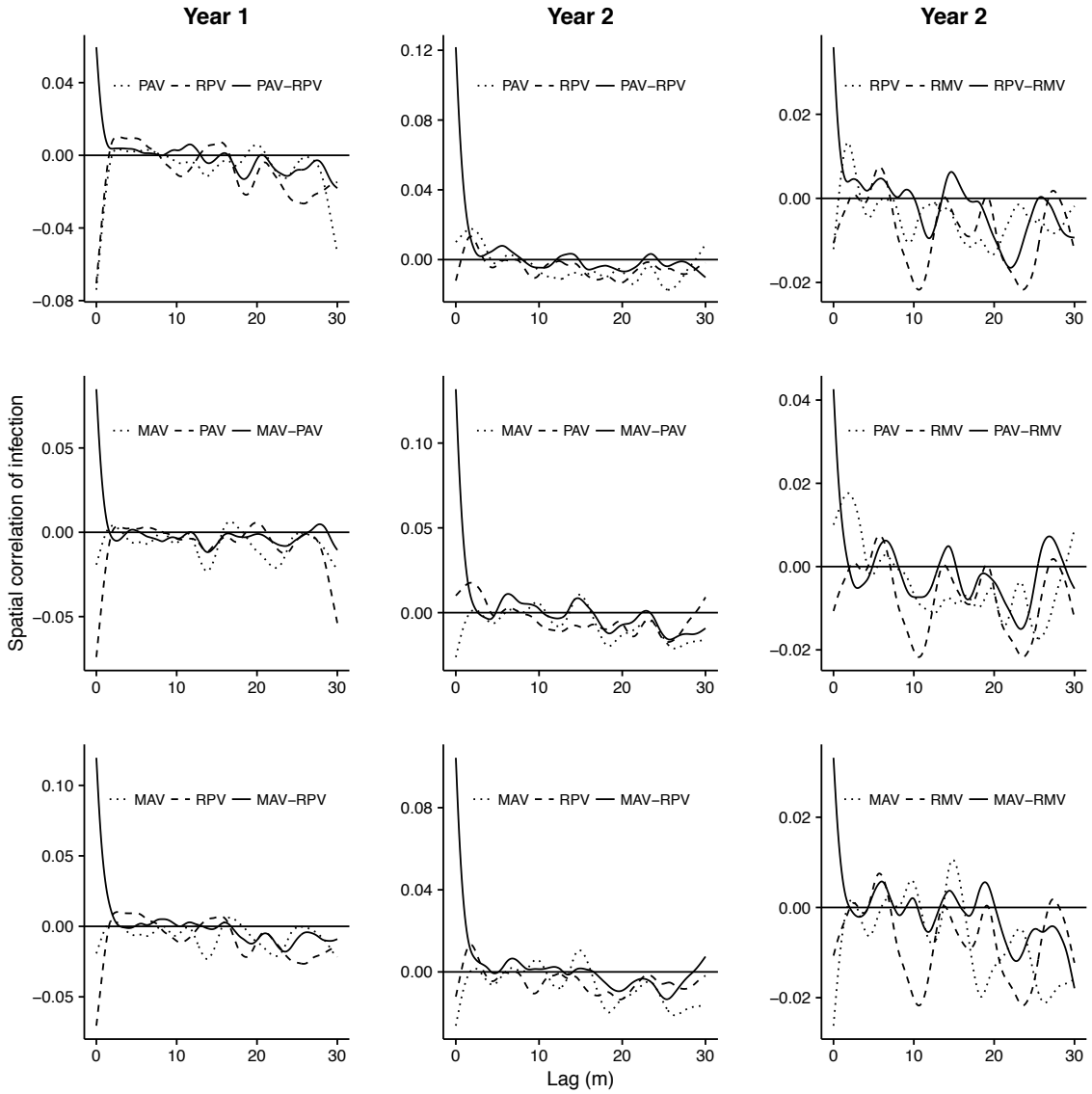

Figure A3. Cross-correlograms for each virus pair in 2007 (first column) and 2008 (second and third columns) along with correlograms for each virus involved in the pair. Mean correlation values across experimental plots are shown. 95% CI are not presented for clarity. Please see Table 2 for information about significance of cross-correlograms. Significant single virus correlograms are shown in Fig. A4 and discussed in the main text.

716 Appendix 4: Single virus autocorrelations with segregation

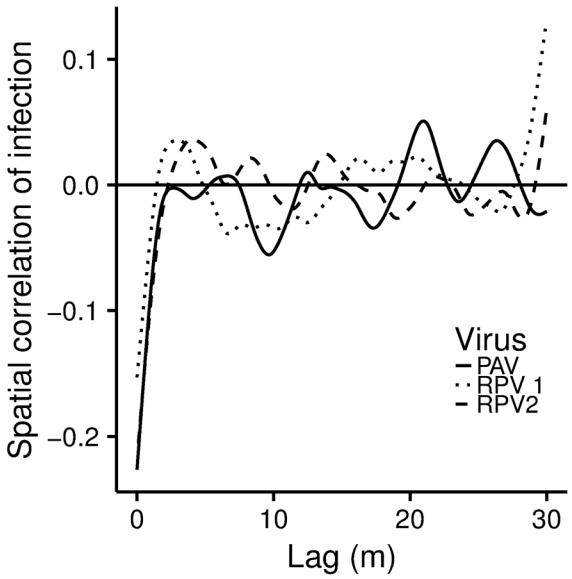

717
718 Figure A4. The three autocorrelations from the first experimental year that had non-
719 random spatial patterns. 95% CI are excluded for clarity. Numbers following "RPV"
720 indicate different experimental plots.
721

Appendix 5: Linear model for vector-sharing and aggregation

Table A5. Linear coefficients, standard error, and P-values for fixed effects and variance of random effects for model testing the effect of vector sharing on the frequency of aggregation between virus pairs in the second experimental year (generalized linear mixed-effects model, logit-link). P-value for "Vector sharing" was obtained from a likelihood ratio test comparing this model with the intercept-only model. Data included 207 observations.

	Estimate (fixed) or Variance (random)	Standard Error	P-value
Fixed effects			
Intercept	-3.6	1.2	0.003
Vector sharing	2.84	0.90	0.003
Random effects			
Viruses:site	2.14		
Site	4.38		

Appendix 6: Linear model for PAV and RPV aggregation

Table A6. Linear coefficients, standard error, and P-values for model testing the effects of nutrient addition, spatial variation in aphid preference, spatial variation in experimental plant weight, and perennial grass percent cover on the frequency of aggregation between PAV and RPV in the second experimental year (generalized linear model, logit-link). Only the significant predictor variables following backwards stepwise selection are included in the table. P-values for predictor variables were obtained from a likelihood ratio test comparing this model with one lacking the focal variable. Model df = 34.

	Estimate	Standard Error	P-value
Intercept	-4.6	1.7	0.006
P addition	2.4	1.0	0.007
Heterogeneity in aphid preference	2.8	1.4	0.02
Perennial grass percent cover	0.056	0.023	0.005